Identification of true microstructure of composites based on various flax fibre assemblies by means of three-dimensional tomography

Miettinen, Arttu; Joffe, Roberts; Pupure, Liva ; Madsen, Bo

Published in:
Proceedings of the 20th International Conference on Composite Materials

Publication date:
2015

Document Version
Publisher's PDF, also known as Version of record

IDENTIFICATION OF TRUE MICROSTRUCTURE OF COMPOSITES BASED ON VARIOUS FLAX FIBRE ASSEMBLIES BY MEANS OF THREE-DIMENSIONAL TOMOGRAPHY

Arttu Miettinen[1], Roberts Joffe[2, 3], Liva Pupure[2] and Bo Madsen[4]

[1]University of Jyvaskyla, Department of Physics, P.O. Box 35, FI-40014 Jyvaskyla, Finland
Email: arttu.miettinen@phys.jyu.fi, web page: http://www.phys.jyu.fi

[2]Luleå University of Technology, Composite Centre Sweden, SE-97187 Luleå, Sweden
Email: roberts.joffe@ltu.se, liva.pupure@ltu.se, web page: http://www.ltu.se/centres/CCSWE

[3]Swerea SICOMP, P.O. Box 271, S-94126 Piteå, Sweden
Web page: http://www.swerea.se/sicomp

[4]Technical University of Denmark, Department of Wind Energy, P.O. Box 49, DK-4000 Roskilde, Denmark
Email: boma@dtu.dk, web page: http://www.vindenergi.dtu.dk

Keywords: Tomography, Flax, Natural fibres, Microstructure

ABSTRACT

Lately it has been demonstrated that natural fibres may be an environmentally superior alternative for, e.g., glass fibres. In order to estimate properties of composite materials made of natural fibres, models designed for synthetic fibres are often used. The models usually do not account for irregularities in the material, e.g., suboptimal fibre orientation due to the twisting angle of fibres in yarns. Use of models without taking those features into account might lead to unreliable results. Methods to quantify the microstructural properties of natural fibre composites with X-ray microtomography and three-dimensional image analysis are demonstrated in this work. The methods are applied to flax fibre composites made from three different kinds of pre-forms. Microstructural parameters estimated with the methods are used in micromechanical models for the stiffness of the composite. Comparison between rule-of-mixtures and classical laminate theory is made, highlighting the requirement for accurate parameter estimation and use of a model that accounts for significant structural features of the material.

1 INTRODUCTION

Natural fibres (NF) are emerging as lightweight and environmentally superior alternatives to glass fibre (GF) for reinforcement in polymer composites. It has been demonstrated that some of NFs (e.g. hemp or flax) have good mechanical properties which are comparable (or even better) than those of GFs, especially if properties normalized with density are considered [1]. Moreover, recently a number of companies have started to produce various types of fabrics based on NF (e.g. woven and non-crimp fabrics) which are very well suited for manufacturing of lightweight, environmentally friendlier, structural composites. In order to design such composite materials, models (e.g. micromechanical models, classical laminate theory) developed for synthetic fibres and polymers are employed. Since NFs are assembled in fabrics with fairly regular meso-structure, it is often assumed in those models that the fibres are continuous and aligned. But even when assembled in bundles and fabrics, NFs are not as well oriented and as regularly distributed as continuous synthetic fibres would be. The actual microstructure of NF composites contains irregularities on different size scales and the use of models without taking these features into account might therefore produce unreliable results which are unusable for further design of structures.

Typically, the microstructural and geometrical parameters of composites are identified from microscopy of polished cross-sections. This is time-consuming and may not be accurate because polishing may remove important features of the microstructure (e.g. voids), affect the geometry of fibres as well as introduce defects and damage. Furthermore, since NFs are rather soft and very sensitive to moisture, conventional polishing techniques cannot readily be used and in most cases polished surfaces of high quality are difficult to obtain.

An alternative non-destructive technique is X-ray microtomography (CT) which gives a three-dimensional (3D) description of the microstructure [1]. It is based on taking a large number of X-ray projection images of the sample in various directions. A three-dimensional matrix of effective local X-ray attenuation coefficients is computationally reconstructed based on the projection images. As the attenuation coefficient correlates with the density of the material, the reconstructed data can be viewed as a 3D image of the sample. In the 3D image value of each voxel is proportional to the density of the material in that voxel. Contrast between regions of different densities, e.g., fibres, matrix and air, is thus produced.

The current paper demonstrates the capabilities of the CT method and image processing algorithms [3, 4] applied to composites manufactured by the vacuum infusion method from different types of flax fibre fabrics, viz. unidirectional fabric obtained by filament winding of dry fibre roving, woven fabric and non-crimp fabric. Image analysis methods are used to characterize the microstructure and damage in the composites. The results of the analysis are used to predict stiffness of the composites and a comparison with mechanical tests is performed.

2 MATERIALS

Three types of flax fibre/Envirez laminates with $[0/90]_S$ lay-up were manufactured with vacuum infusion method from three types of pre-forms. The first pre-form was produced from unidirectional non-crimp fabric (NCF), the second one from woven fabric (W) and the third one from unidirectional fabric obtained by filament winding of dry fibre roving (FW).

The stiffness of the flax fibres (E_f) in FW and in NCF was estimated to be 69 GPa and 50 GPa, respectively. The stiffness of matrix was E_m = 3.4 GPa. The axial stiffness of unidirectional and cross-ply laminates (E_L and E_X, respectively) along with Poisson's ratio (ν_{LT}) were measured experimentally from tensile tests. The shear modulus (G_{LT}) was measured from tensile tests of [±45] laminates. The properties of the composites are shown in Table 1**.**

For comparison purposes, the fibre volume fraction was obtained by image analysis from microscope images of cross-section of unidirectional laminate by simple thresholding (see Fig. 1). Properties of W composite are not presented as it was not used for demonstrating micromechanical modelling.

Material	V_f^{CT}	η_o	V_f^{OM}	E_L [GPa]	E_X [GPa]	G_{LT} [GPa]	ν_{LT}
NCF	0.31	0.75	0.40	13.1	8.2	1.8	0.482
W	0.31	0.83	-	-	-	-	-
FW	0.32	0.90	0.28	20.5	12	1.8	0.398

Table 1: Properties of composites. V_f^{CT} denotes volume fraction of fibres as measured with CT; V_f^{OM} denotes volume fraction of fibres as measured with optical microscopy; η_o denotes orientation efficiency factor of zero-degree layer as measured with CT; E_L, E_X, G_{LT} and ν_{LT} denote Young's modulus of unidirectional composite, Young's modulus of cross-ply laminate, shear modulus of composite and Poisson's ratio of composite as measured with tensile tests, respectively.

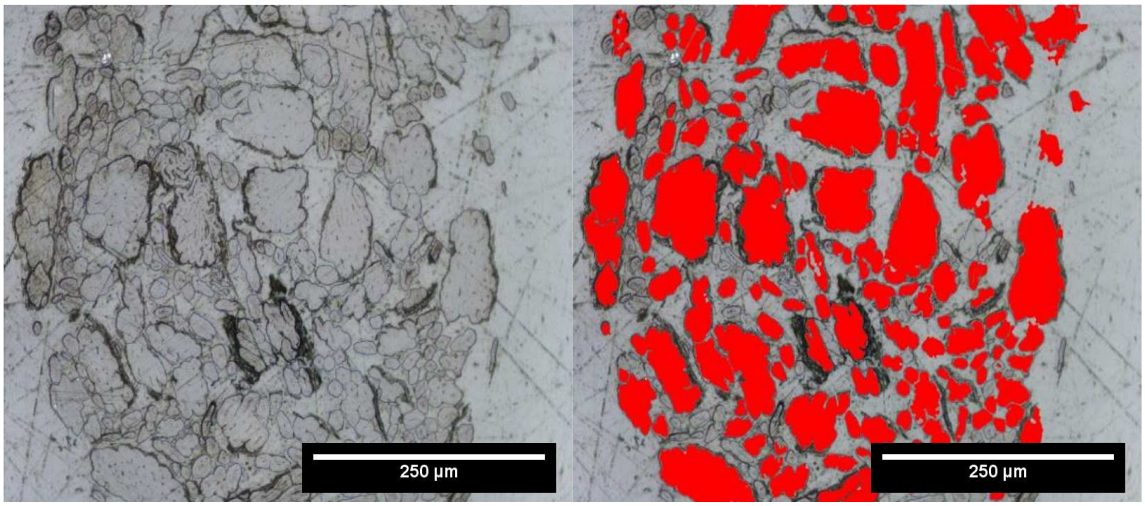

Figure 1: Optical microscopy image used for determination of fibre volume fraction (left) along with processed image (right) showing accounted fibres shaded in red.

3 X-RAY MICROTOMOGRAPHY AND IMAGE ANALYSIS

To prepare specimens of NCF, W and FW composites for X-ray microtomographic imaging, subsamples of approximately 2.6 mm × 5 mm × 5 mm were carefully cut from each specimen using a hand saw. The subsamples were taken from the central part of each specimen (after tensile test), ensuring that a part of the fracture surface was represented in each subsample. The subsamples were CT scanned with Xradia µCT-400 device, applying 30 kV acceleration voltage and 3 W X-ray power. 1783 projection images with 2.8 µm pixel size and 15 s exposure time per projection image were collected over 180 degrees of rotation.

After reconstruction, a 3D Gaussian filter ($\sigma = 0.5$ pixels) was applied to the reconstructed slices to attenuate imaging noise (Fig. 2). Contrast-to-noise ratio between background and matrix was found to be greater than 10 and between matrix and fibres greater than 6. The different phases could thus be easily separated from each other by simple thresholding, yielding three binary images: one containing only the fibres, one containing only the matrix and one containing only voids and cracks. The volume of objects in the binary images were determined and used to calculate the volume fraction of fibres (Table 1).

In the present materials, the individual fibres are attached to each other forming bundles that in turn form yarns. In the NCF composite the yarns have approximately circular cross-section and the fibre bundles have been twisted around each other. To quantify the twisting angle, the individual yarns in the binary image of fibres were manually separated from each other. The separated yarns were processed one cross-sectional slice at a time. First, the geometrical centre point $\vec{c}_i$ of fibre cross-section in the i:th cross-sectional slice was found. The cross-sectional slice was compared to the next one using a digital image correlation technique. The result of the image correlation algorithm was a displacement field $\vec{u}_i(x, y)$ required to deform the i:th cross-sectional slice into $i + 1$:th cross-sectional slice. After converting $\vec{u}_i(x, y)$ into polar coordinates $\vec{u}_i(r, \theta)$ around $\vec{c}_i$, the local twisting rate around $\vec{c}_i$ is given by

$$\omega_i(r, \theta) = \frac{\vec{r}(r, \theta) \times \vec{u}_i(r, \theta)}{r^2 \Delta_i}, \tag{1}$$

where $\vec{r}$ is the position vector and Δ_i is the spacing between the two consecutive cross-sectional slices. Averaging over θ and all cross-sectional slices then results in $\omega(r)$, twisting rate as a function of distance from yarn centreline. The twisting angle is then

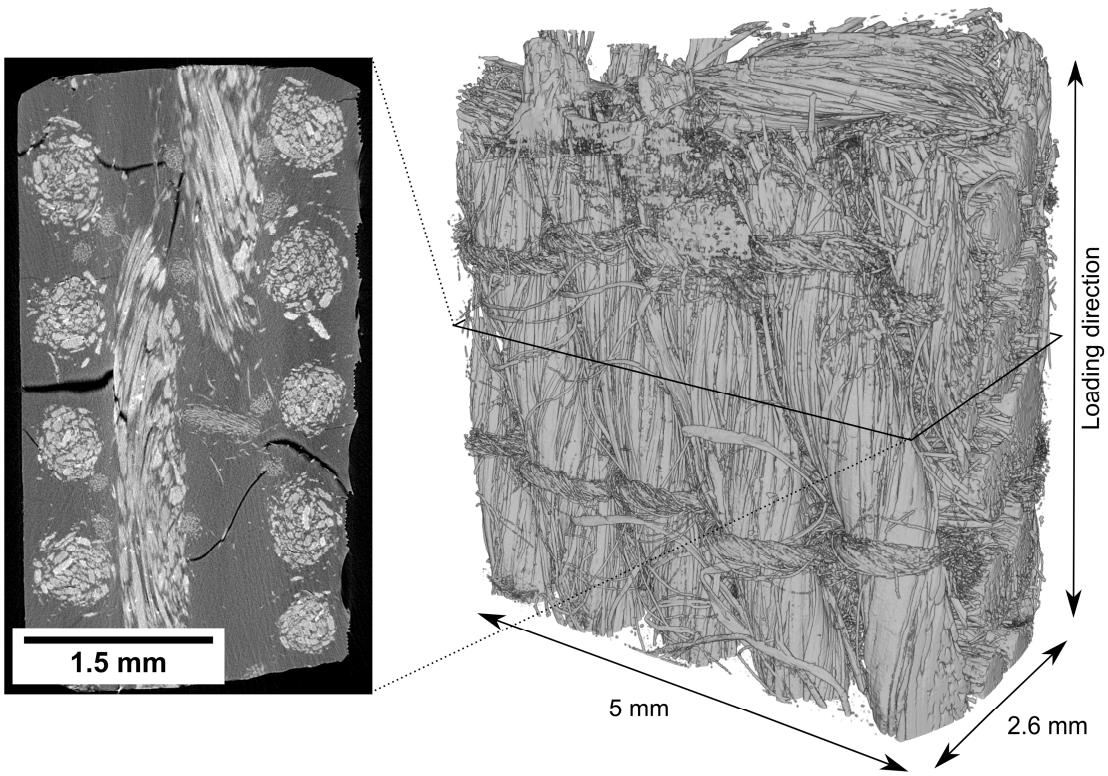

Figure 2: A single cross-sectional CT slice through NCF composite (left), featuring air (black), matrix (grey) and fibres (nearly white). Visualization of fibres in a CT image of NCF composite (right).

$$\beta(r) = \operatorname{atan}\left(\frac{2\pi r}{L(r)}\right), \tag{2}$$

where $L(r) = 2\pi/\omega(r)$ is the twist of the yarn, i.e., the length required for the yarn to turn once around itself. This definition of twisting angle corresponds to that in [5]. The twisting angles of some yarns in NCF are drawn in Fig. 3.

To facilitate determination of yarn diameter at its i:th cross-section, an azimuthal average $f_i(r)$ of the cross-sectional slice was determined with $\vec{c}_i$ as the center point. The diameter was then taken to be twice the smallest radius that satisfies $f_i(r) < \bar{f}_i/2$, where $\bar{f}_i$ is the median of $f_i(r)$. Statistical binning of diameters at all cross-sectional slices gives the diameter distribution of the yarn (Fig. 3).

Orientation of fibres was determined using the structure tensor method [6]. The method is based on determining the local structure tensor, whose components are given by

$$S_{ij}(\vec{x}) = \left(G_{\sigma_t} * I_i I_j\right)(\vec{x}), \tag{3}$$

where G_σ is a three-dimensional Gaussian function with zero mean and standard deviation σ, $*$ denotes convolution, and

$$I_i = \frac{\partial G_{\sigma_s}}{\partial x_i} * I \tag{4}$$

is an approximation of the i:th partial derivative of the binary image of fibres $I(\vec{x})$. The eigenvector corresponding to the smallest eigenvalue of $S_{ij}(\vec{x})$ is taken as an estimate of the local fibre orientation at $\vec{x}$. As the loading direction of the composite sample is known, the angle α between the local fibre orientation and the loading direction can be calculated. Statistical binning of the values of α at all fibre voxels gives the orientation distribution of fibre volume (Fig. 3). The Krenchel orientation efficiency factor η_o [7] was then determined as

$$\eta_o = \frac{\sum_i V_{\alpha_i} \cos^4 \alpha_i}{\sum_i V_{\alpha_i}}, \tag{5}$$

where V_{α_i} is the volume fraction of fibres whose angle to the loading direction is α_i. As orientation efficiency factor is needed for the zero-degree layers only (see Section 4), the sums were taken over bins with $\alpha_i \in [0^\circ, 45^\circ]$, corresponding to fibres in the zero-degree layers. The orientation efficiency factors are shown in Table 1.

The crack opening displacement was determined from the binary image of cracks with the local thickness transform [8]. The local thickness transform assigns to each crack voxel the diameter of the largest sphere that fits into the crack and contains the voxel. The distribution of voxel values in the transformed image is the thickness distribution of crack volume that is identified as the distribution of crack opening displacement. By considering only voxels at the edge of the specimen, distribution of crack opening displacement at the edge can also be determined (Fig. 3).

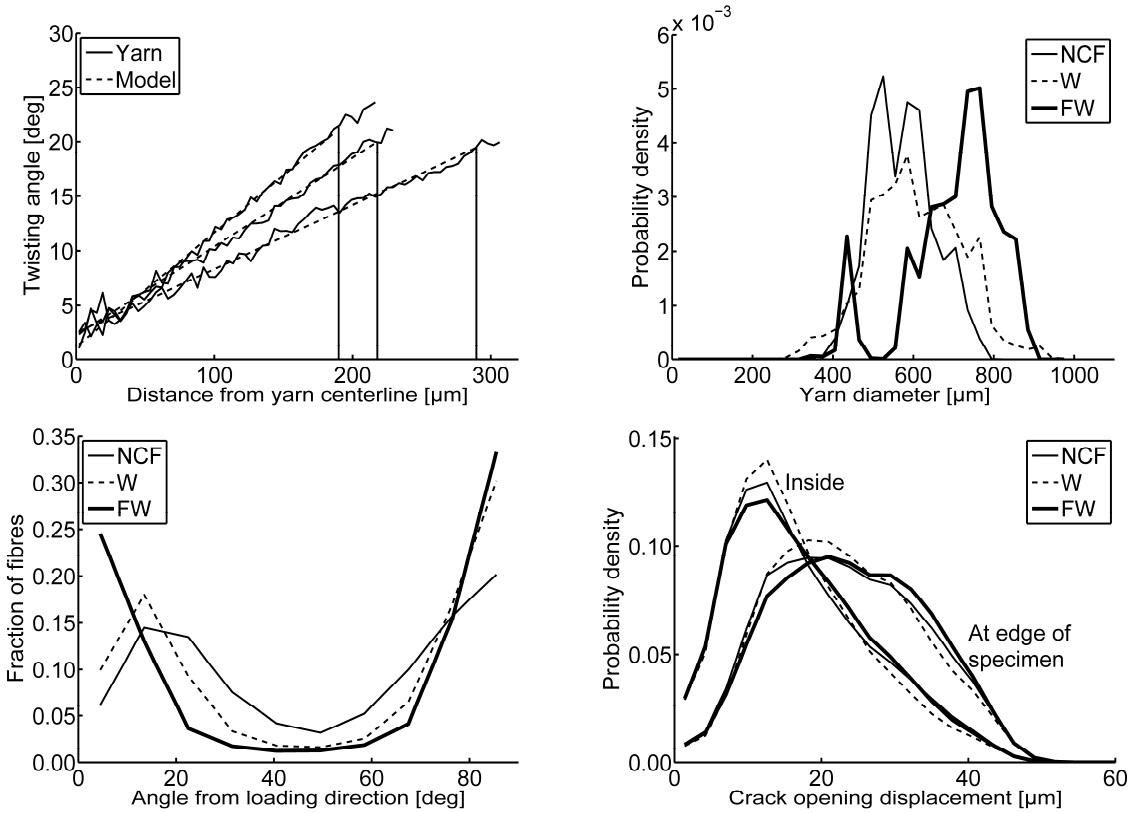

Figure 3: Yarn twisting angle in three yarns of NCF composite, along with fitted model from [5], and yarn diameters plotted with vertical lines (top-left), yarn diameter distributions (top-right), fibre orientation distributions (bottom-left) and crack opening displacement (bottom-right).

4 MICROMECHANICAL MODELLING

As an initial estimate, the longitudinal and transverse Young's modulus (E_L and E_T, respectively) of an unidirectional layer were calculated by use of rule-of-mixtures (RoM) as

$$E_L = V_f E_f + (1 - V_f) E_m, \tag{6}$$

$$E_T = \left(\frac{V_f}{E_{f,T}} + \frac{1 - V_f}{E_m} \right)^{-1}, \tag{7}$$

where $E_{f,T}$ is the transverse Young's modulus of fibres. As $E_{f,T}$ was not measured independently, it was assumed that $E_{f,T} \approx E_f/7$ based on results reported in [9] for jute fibre. Finally, the Young's modulus of the cross-ply laminate with lay-up $[0/90]_S$ was calculated as

$$E_X = \frac{1}{2}(E_L + E_T). \tag{8}$$

The results of the model (Eq. 8) with V_f determined by optical microscopy (see Table 1) are shown in Fig. 4 with dark grey bars.

In the CT method, information about the orientation of fibres is also available and to account for it, Eq. 6 was modified into

$$E_L = \eta_o V_f E_f + (1 - V_f) E_m, \tag{9}$$

where η_o is the orientation efficiency factor defined in Eq. 5. Equations 7 and 8 were not modified. The results given by the model, with V_f and η_o determined by CT, are shown in Fig. 4 with light grey bars.

Finally, the longitudinal Young's moduli of the composites were estimated using classical laminate theory. In order to facilitate the calculation, the orientation distribution of the composite (see Fig. 3) was divided into ten bins. Each bin was associated with a unidirectional ply where fibre orientation was in the direction corresponding to the bin. Ply thickness was assigned according to the volume fraction of fibres in the particular orientation. The resulting lay-up was considered to form one half of a symmetric laminate. It was used to calculate the Young's modulus of the laminate with LAP software (Anaglyph Ltd, UK). The results of the calculations are shown in Fig. 4 with white bars.

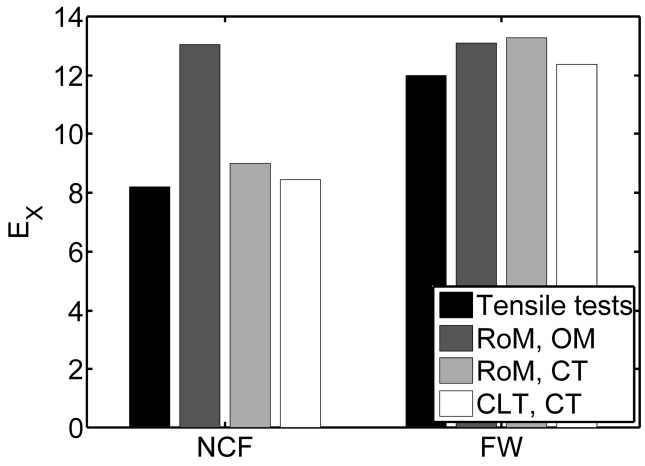

Figure 4: Young's modulus of the NCF and FW composites as determined by mechanical tests (black bars) and by micromechanical models. RoM stands for rule-of-mixtures, CLT for classical laminate theory, OM for parameter estimation by optical microscopy and CT for parameter estimation by computed tomography.

5 RESULTS AND DISCUSSION

In [5] it has been assumed that twisting angle of fibres in ring spun yarn increases linearly in distance from yarn centreline. Based on measured twisting angles shown in Fig. 3 one may conclude that the relation between distance from yarn centreline and twisting angle is indeed linear. However, there seems to be an offset in the twist at zero distance, pointing out that the fibres twist even at the geometrical centre of yarn cross-section. This highlights that the centre of rotation may not lie exactly at the geometrical centre of the yarn cross-section.

Based on Fig. 4 (dark grey bars) it is evident that the Young's moduli calculated with RoM using volume fraction determined with optical microscopy are higher than the values from tensile tests. The difference between value from tensile test and RoM result for FW composite is approximately 10 %, whereas in the case of NCF the difference is very significant and exceeds 60 %. There are several possible sources for this discrepancy related to inaccuracy in parameters of microstructure of the composite, such as fibre discontinuities, fibre orientation, fibre volume fraction and porosity.

The length of flax fibres is usually within the interval of 10 mm – 40 mm, whereas the typical diameter of flax fibre is 10 µm – 40 µm. Thus, aspect ratio of fibres is over 1000, which for practical purposes means that the fibres can be assumed to be made of continuous filament. Thus it is concluded that fibre discontinuities should not have a major effect on the RoM results in this case.

The RoM used for calculation of stiffness (Eqs. 6 – 8) assumes perfect unidirectional orientation of fibres. However, in order to keep filaments together within the roving, the fibres are twisted. In case of roving used for filament winding the twist is low but in order to produce NCF fibre bundles are highly twisted. Thus, fibre orientation is not perfect and may deviate from the direction of loading.

Fibre volume fraction was obtained from image analysis of composite cross-sections similar to those shown in Fig. 1. As seen from the image the flax fibres are highly irregular in shape, moreover, as seen from processed image (on the right) some of the fibres are discarded due to poor contrast. Thus it is suspected that the fibre volume fraction measurements may be inaccurate.

Orientational effects and uncertainty in volume fraction of fibres was accounted for in Eq. 9 with Krenchel orientation efficiency factor and by estimating volume fraction of fibres from CT images. The estimates of Young's modulus calculated using RoM model with these modifications (Fig. 4, light grey bars) are approximately 10 % higher than the results of tensile tests, for both composites. The improvement over RoM model without orientation efficiency factor and with uncertain volume fraction is clear.

Finally, the Young's moduli calculated using classical laminate theory (Fig. 4, white bars) are approximately 3 % higher than the results from tensile tests. Such a deviation is easily explained by uncertainties in the mechanical and microstructural parameters and by the fact that porosity has not been accounted for.

Analysis of the fibre orientation distributions presented in Fig. 3 supports the previous results which showed that calculated Young's modulus for NCF laminate differed from experimental results much more significantly than that of FW composite, when fibre orientation was not accounted for. Indeed, the fraction fibres with orientation of 0˚ – 10° and 80˚ – 90° for FW laminate is 37.5 % and 49 %, whereas for NCF laminate the fractions are 20.5 % and 36 %, respectively. This is in agreement with the fact that yarns in FW are only slightly twisted, whereas yarns in NCF have very high twist.

The values of the orientation efficiency factors in Table 1 also suggest the same conclusions about orientational structure of the composites. In that sense yarns in W seem to fall in between of NCF and FW. Based on visual inspection of the CT images, the yarns in W have no clear twist, but the fibre orientation deviates from the ideal 0˚/90˚ configuration due to the weave pattern. The weave pattern does not occur in FW and thus the fibres are more ideally oriented than those in W.

Yarn diameter distributions in Fig. 3 show that yarns in NCF are the thinnest of the three, whereas yarns in FW are the thickest. To achieve approximately same volume fraction, fibre bundles in yarns of NCF must be more tightly packed than those in the two other composites. Thus, in NCF there are larger reinforcement-free volumes that may cause uneven stress distribution.

Although the mechanical properties and the microstructure of the three composites seem to differ from each other, their cracking behaviour seems to be similar. The crack opening displacement distributions of the three composites (Fig. 3) are nearly identical, both inside the specimen and at the

surface of the specimen. It should be noted that the cracks studied in this work are not produced in fatigue cracking but in simple tensile test. Thus, conclusions might be different if fatigue cracking was studied, but similar image analysis procedures could be used in that case, too.

6. SUMMARY

CT methods for determination of microstructural parameters of flax fibre composite materials were demonstrated. In particular, focus was on properties related to micromechanical modelling. The stiffness of two of the composites was calculated with a rule-of-mixtures model and, for comparison, with classical laminate theory, with microstructural parameters measured from the CT images. The results were compared to mechanical tests and to RoM calculations made with microstructural parameters estimated from optical micrographs. The results show that if orientation of fibres is not accounted for, the rule-of-mixtures model may give significantly over-predicted estimates of stiffness, especially for laminates containing yarns with high twisting angle. Calculations based on CLT with microstructural parameters extracted from CT images seemed to be the most accurate. The remaining inaccuracy may be attributed to porosity, which was not accounted for.

ACKNOWLEDGEMENTS

Colleagues Newsha Doroudgarian (LTU), Runar Långström (Swerea SICOMP) and project course students (T7009T course at LTU 2013-2014 LP1-2) Michael Kraus and Mostafa Ismail are acknowledged for their help with manufacturing of the composites and performing the experiments.

REFERENCES

[1] E. Spārniņš, *Mechanical properties of flax fibers and their composites*, doctoral thesis, Luleå University of Technology, 2009.

[2] A. C. Kak, M. Slaney, *Principles of computerized tomographic imaging*, IEEE Press, New York, 1988.

[3] A. Miettinen, A. Ojala, L. Wikström, R. Joffe, B. Madsen, K. Nättinen, M. Kataja, Non-destructive automatic determination of aspect ratio and cross-sectional properties of fibres, *submitted to Composites Part A*, 2015.

[4] A. Miettinen, C. L. Luengo Hendriks, G. Chinga-Carrasco, E. K. Gamstedt, M. Kataja, A non-destructive X-ray microtomography approach for measuring fibre length in short-fibre composites, *Composites Science and Technology*, **72**, 2012, pp. 1901-1908, (doi: 10.1016/j.compscitech.2012.08.008)

[5] B. Madsen, P. Hoffmeyer, A. B. Thomsen and H. Lillholt, Hemp yarn reinforced composites – I. Yarn characteristics, *Composites Part A*, **38**, 2007, pp. 2194-2203 (doi: 10.1016/j.compositesa.2007.06.001).

[6] B. Jähne, *Practical Handbook on image processing for scientific and technical applications*, Second edition, CRC Press, Heidelberg, 2004.

[7] H. Krenchel, *Fibre reinforcement*, Technical University of Denmark, Copenhagen, 1964.

[8] T. Hildebrand and P. Rüegsegger, A new method for the model-independent assessment of thickness in three-dimensional images, *Journal of Microscopy*, **185**, 1997, pp. 67-75 (doi: 10.1046/j.1365-2818.1997.1340694.x).

[9] F. R. Cichocki Jr. and J. L. Thomason, Thermoelastic anisotropy of a natural fiber, *Composites Science and Technology*, **62**, 2002, pp. 669-678 (doi: 10.1016/S0266-3538(02)00011-8).